Possible Charge-Density-Wave/Spin-Density-Wave in the Layered Pnictide−Oxides: $Na_2Ti_2Pn_2O$ (Pn = As, Sb)

Tadashi C. Ozawa and Susan M. Kauzlarich*

Department of Chemistry, One Shields Avenue, University of California Davis, Davis, California 95616

Mario Bieringer and John E. Greedan

Institute for Materials Research, McMaster University, Hamilton, Ontario L8S 4M1, Canada

Received January 4, 2001. Revised Manuscript Received March 8, 2001

The compounds $Na_2Ti_2Pn_2O$ (Pn = As, Sb) crystallize in the anti-K_2NiF_4 structure type in the space group, $I4/mmm$, with $Z = 2$ and the lattice parameters $a = 4.0810(9)$ Å and $c = 15.311(3)$ Å for the As analogue at 310 K and $a = 4.160(2)$ Å and $c = 16.558(7)$ Å for the Sb analogue at 150 K. The structure consists of edge-shared $^2_\infty[Ti_{4/2}Pn_2O_{4/4}]^{2-}$ layers separated by double layers of Na^+. These compounds exhibit an anomalous transition in the temperature-dependent magnetic susceptibility at $T_c^{onset} = 330$ K for the As analogue and $T_c^{onset} = 120$ K for the Sb analogue. Temperature-dependent powder neutron diffraction has been performed to investigate the magnetic spin ordering and structure symmetry breakdown of the compounds; however, no scattering due to magnetic spin ordering or symmetry change has been detected. The temperature-dependent electrical resistivity of these compounds also exhibits an anomaly reminiscent of CDW (charge-density-wave)/SDW (spin-density-wave) materials. The As analogue shows an insulator-to-insulator transition around 135 K whereas the Sb analogue shows a metal-to-metal transition around 120 K that corresponds well to the onset of the anomaly in the magnetic susceptibility. The similarity and difference in the physical properties between the As and Sb analogues as well as related compounds will be discussed.

Introduction

Recently, there have been extensive studies on layered transition metal suboxides, such as pnictide−oxides[1−21] and oxychalcogenides.[22−30] In these compounds, pnictogen, chalcogen, and oxygen all exist as anions. Because of this mixed anionic environment, suboxides tend to have unique structures that are rarely observed in simple oxide materials. For instance, many mixed-layer compounds have been discovered in pnictide−oxides[1−10] and oxychalcogenides[28−30] where the structure consists of $ThCr_2Si_2$-type metal−pnictide or metal−chalcogenide layers alternating with CuO_2^{2-}-type square planar metal−oxide layers. Among the suboxides, those with layered structure types are of particular interest because the physical properties are

* To whom correspondence should be addressed.

(1) Brechtel, E.; Cordier, G.; Schäfer, H. *Z. Naturforsch. B* **1979**, *30*, 777.
(2) Stetson, N. T.; Kauzlarich, S. M. *Inorg. Chem.* **1991**, *30*, 392.
(3) Brock, S. L.; Kauzlarich, S. M. *Inorg. Chem.* **1994**, *33*, 2491.
(4) Brock, S. L.; Kauzlarich, S. M. *Chem. Tech.* **1995**, *25*, 18.
(5) Brock, S. L.; Kauzlarich, S. M. *Comments Inorg. Chem.* **1995**, *17*, 213.
(6) Brock, S. L.; Kauzlarich, S. M. *J. Alloys Compd.* **1996**, *241*, 82.
(7) Brock, S. L.; Raju, N. P.; Greedan, J. E.; Kauzlarich, S. M. *J. Alloys Compd.* **1996**, *237*, 9.
(8) Ozawa, T.; Olmstead, M. M.; Brock, S. L.; Kauzlarich, S. M.; Young, D. M. *Chem. Mater.* **1998**, *10*, 392.
(9) Matsushita, A.; Ozawa, T. C.; Tang, J.; Kauzlarich, S. M. *Physica B* **2000**, *284−288*, 1424.
(10) Enjalran, M.; Scalettar, R. T.; Kauzlarich, S. M. *Phys. Rev. B* **2000**, *61*, 14570.
(11) Brechtel, E.; Cordier, G.; Schäfer, H. *Z. Naturforsch. B* **1981**, *86*, 27.
(12) Eisenmann, B.; Limartha, H.; Schäfer, H. *Z. Naturforsch. B* **1980**, *35*, 1518.
(13) Adam, A.; Schuster, H.-U. *Z. Anorg. Allg. Chem.* **1990**, *584*, 150.
(14) Kaczorowski, D.; Albering, J. H.; Noël, H.; Jeitschko, W. *J. Alloys Compd.* **1994**, *216*, 117.
(15) Cava, R. J.; Zanbergen, H. W.; Krajewski, J. J.; Siegrist, T.; Hwang, H. Y.; Batlogg, B. *J. Solid State Chem.* **1997**, *129*, 250.
(16) Axtell, E. A., III.; Ozawa, T.; Kauzlarich, S. M.; Singh, R. R. P. *J. Solid State Chem.* **1997**, *134*, 423.
(17) Diot, N.; Marchand, R.; Haines, J.; Léger, J. M.; Macaudière, P.; Hull, S. *J. Solid State Chem.* **1999**, *146*, 390.
(18) Charkin, D. O.; Berdonosov, P. S.; Dolgikh, V. A.; Lightfoot, P. *J. Alloys Compd.* **1999**, *292*, 118.
(19) Quebe, P.; Terbüchte, L. J.; Jeitschko, W. *J. Alloys Compd.* **2000**, *302*, 70.
(20) Ozawa, T. C.; Pantoja, R.; Axtell, E. A., III.; Kauzlarich, S. M.; Greedan, J. E.; Bieringer, M.; Richardson, J. W., Jr. *J. Solid State Chem.* **2000**, *153*, 275.
(21) Brock, S. L.; Hope, H.; Kauzlarich, S. M. *Inorg. Chem.* **1994**, *33*, 405.
(22) Deudon, C.; Meerschaut, A.; Cario, L.; Rouxel, J. *J. Solid State Chem.* **1995**, *120*, 164.
(23) Cody, J. A.; Deudon, C.; Cario, L.; Meerschaut, A. *Mater. Res. Bull.* **1997**, *32*, 1181.
(24) Cario, L.; Deudon, C.; Meerschaut, A.; Rouxel, J. *J. Solid State Chem.* **1998**, *136*, 46.
(25) Zhu, W. J.; Hor, P. H. *J. Solid State Chem.* **2000**, *153*, 26.
(26) Zhu, W. J.; Hor, P. H. *J. Solid State Chem.* **1997**, *134*, 128.
(27) Zhu, W. J.; Hor, P. H. *Inorg. Chem.* **1997**, *36*, 3576.
(28) Zhu, W. J.; Hor, P. H.; Jacobson, A. J.; Crisci, G.; Albright, T. A.; Wang, S. H.; Vogt, T. *J. Am. Chem. Soc.* **1997**, *119*, 12398.
(29) Zhu, W. J.; Hor, P. H. *J. Solid State Chem.* **1997**, *130*, 319.
(30) Otzschi, K.; Ogino, H.; Shimoyama, J.; Kishio, K. *J. Low Temp. Phys.* **1999**, *117*, 729.

10.1021/cm010009f CCC: $20.00
Published on Web 04/20/2001

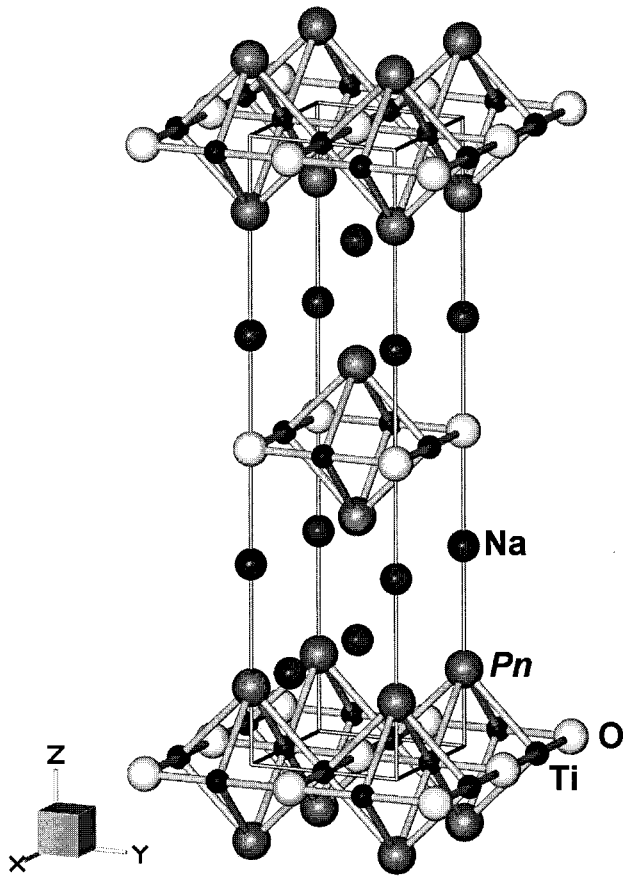

Figure 1. Crystal structure of $Na_2Ti_2Pn_2O$ (Pn = As, Sb) showing alternation of $^2_\infty[Ti_{4/2}Pn_2O_{4/4}]^{2-}$ layers and double layers of Na^+.

affected by both inter- and intralayer interactions. Furthermore, theoretical physics of layered compounds is relatively well established; thus, experimentally observed features can be compared with the theoretical models to further the understanding of the structure−property relationships.

$Na_2Ti_2Pn_2O$ (Pn = As, Sb) are layered pnictide−oxide compounds that were first discovered by Adam et al. in the early 1990s.[13] To our knowledge, this is the only pnictide−oxide containing Ti^{3+}, a d^1 transition metal. Geometrically, the structure of $Na_2Ti_2Pn_2O$ (Figure 1) is the K_2NiF_4 type, which is also seen in cuprate high-T_c superconductors such as $La_{2-x}Ba_xCuO_{4-\delta}$.[31] The K_2NiF_4 structure type consists of layers of a vertex-shared octahedral unit, $^2_\infty[NiF_2F_{4/2}]^{2-}$, stacked in a body-centered fashion separated by single layers of K^+ along the *c* axis. This configuration corresponds to $^2_\infty[ONa_2Ti_{4/2}]^{2-}$ layers (Figure 2a) and Pn^{3-} layers of $Na_2Ti_2Pn_2O$ where positions of cations and anions are reversed from those in the K_2NiF_4 type. Thus, the chemical structure of this compound should be classified as the anti-K_2NiF_4 type. In addition, by considering the interatomic distances, oxidation states of each element and Zintl electron counting rule,[32] it is reasonable to view these compounds as edge-shared $^2_\infty[Ti_{4/2}Pn_2O_{4/4}]^{2-}$ layers (Figure 2b) interspersed by double layers of Na^+. In the $[Ti_{4/2}Pn_2O_{4/4}]^{2-}$ unit, Ti^{3+} is located between two O^{2-} forming a square planar layer, $[Ti_{4/2}O]^{4+}$, which is an anticonfiguration to the $[CuO_{4/2}]^{2-}$ layer observed in high-T_c cuprates. There are only a few examples of layered compounds with anti-$[CuO_{4/2}]^{2-}$-type layers; one such example is $Na_{1.9}Cu_2Se_2Cu_2O$.[33] Ti^{3+} is also four-coordinated by Pn^{3-}, forming a $[Ti_2Pn_2O_{4/4}]^{2-}$ unit where Pn^{3-} is located above and below the center of the $[Ti_{4/2}O_{4/4}]^{4+}$ square unit. This Ti coordination of the $[Ti_{4/2}Pn_2O_{4/4}]^{2-}$ unit is also observed in a few rare earth oxysulfides with sulfur replacing the Pn.[22−24]

We have previously measured the temperature-dependent magnetic susceptibility and electrical resistivity of the Sb analogue, $Na_2Ti_2Sb_2O$, and have discovered that this compound exhibits a sharp drop in magnetic susceptibility and a metal-to-metal transition in the electrical resistivity at $T_c \sim 120$ K reminiscent of CDW/SDW materials.[16] In addition, temperature-dependent powder neutron diffraction was performed on this compound to investigate this anomaly.[20] We have found a structure distortion in the $^2_\infty[Ti_{4/2}Sb_2O_{4/4}]^{2-}$ layer coincident with the T_c of magnetic susceptibility and resistivity, suggesting strong electron−phonon interaction as the origin of the anomaly. These investigations of the structure−property relationship of the Sb analogue have generated much interest. For example, the electronic structure of $Na_2Ti_2Sb_2O$ has been studied by two groups,[34,35] and a CDW/SDW as the origin of the physical property anomaly has been suggested. In addition, a theoretical model of the magnetic interaction of Ti^{3+} in this compound has been proposed.[36,37]

In this paper, we report further investigations of the $Na_2Ti_2Pn_2O$ system by synthesizing the bulk sample of the As analogue and comparing its physical properties to that of the Sb analogue. For both Sb and As analogues, electrical resistivity and magnetic susceptibility were measured under various temperatures and magnetic fields. Also, temperature-dependent powder neutron diffraction has been performed. The results from these experiments as well as the effect of Pn^{3-} on the physical properties of the $Na_2Ti_2Pn_2O$ system will be discussed.

Experimental Procedures

Sample Preparation. Polycrystalline samples were prepared by solid-state sintering of Na_2O (Johnson Matthew 98%), Ti (Cerac 99.98%), and As (Johnson Matthey 99.999%) or Sb (Cerac, 99.999%). A preliminary purity check on these starting materials by powder X-ray diffraction indicated that the batch of Na_2O contained a few percent of Na_2O_2 as an impurity phase. Thus, the stoichiometry was adjusted to have the exact Na content in the product as

$$x\mathrm{Na_2O_2} + (100-x)\mathrm{Na_2O} + 200\mathrm{Ti} + 200\mathrm{Pn} \rightarrow 100\mathrm{Na_2Ti_2Pn_2O} + 0.5x\mathrm{O_2}$$

where $1 \le x \le 5$ depends on the batch of the Na_2O used.[20]

(31) Bednorz, J. G.; Müller, K. A. *Z. Phys. B* **1986**, *64*, 189.
(32) Kauzlarich, S. M. In *Chemistry, Structure, and Bonding of Zintl Phases and Ions*; Kauzlarich, S. M., Ed.; VCH: New York, 1996; p 245.
(33) Park, Y.; DeGroot, D. C.; Schinder, J. L.; Kannewurf, C. R.; Kanatzidis, M. G. *Chem. Mater.* **1993**, *5*, 8.
(34) Pickett, W. E. *Phys. Rev. B* **1998**, *58*, 4335.
(35) Fabrizi de Biani, F.; Alemany, P.; Canadell, E. *Inorg. Chem.* **1998**, *37*, 5807.
(36) Pati, S. K.; Singh, R. R. P.; Khomskii, D. I. *Phys. Rev. Lett.* **1998**, *81*, 5406.
(37) Singh, R. R. P.; Starykh, O. A.; Freitas, P. J. *J. Appl. Phys.* **1998**, *83*, 7387.

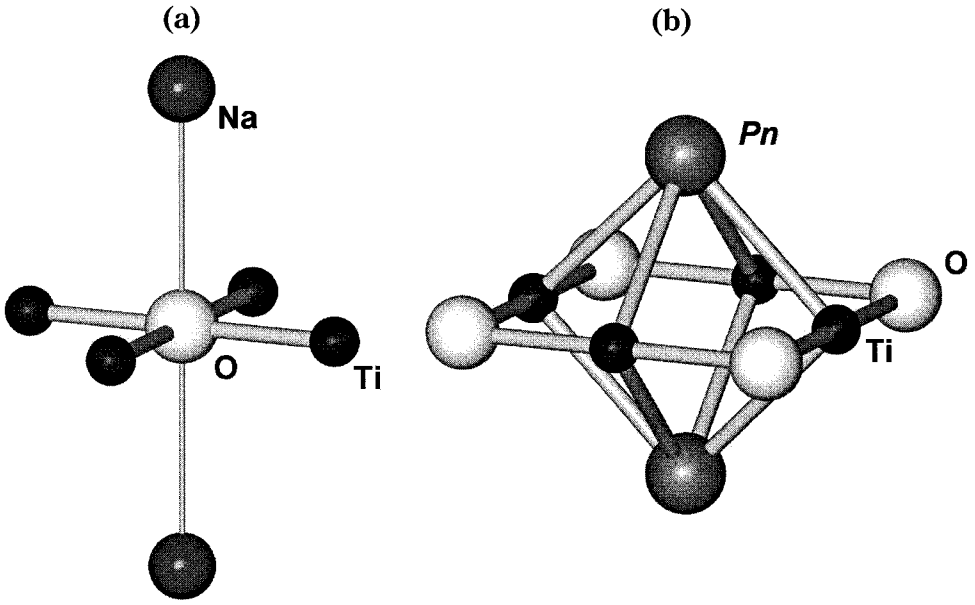

Figure 2. Atomic coordination in $Na_2Ti_2Pn_2O$. (a) Octahedral coordination around O^{2+} where four Ti^{4+} are in the equatorial positions and two Na^+ are in the apical positions. (b) $[Ti_{4/2}Pn_2O_{4/4}]^{2-}$ unit consisting of Ti−O square planar capped with two Pn^{3-}.

This stoichiometric ratio of the starting materials was mixed in an agate mortar in an argon-filled drybox. The resulting powder mixture was pelletized and sealed in a pre-etched Ta tube under nitrogen gas. Finally, the Ta tube was sealed in a fused silica ampule under 1/5 atm of argon. The sample was quickly heated to 1000 °C, held for 3 days, and furnace-cooled. The product retained the pellet shape and had a dark gray color.

Powder X-ray Diffraction. The product purity was checked by powder X-ray diffraction on an Enraf Nonius Guinier camera utilizing Cu $K\alpha_1$ radiation with silicon (NBS SRM 640b) as an internal reference for both As and Sb compounds. The film was scanned and digitized using Film Scan[38] and Jade software.[39] Powder diffraction was also performed on a Siemens D500 X-ray diffractometer at room temperature using Cu Kα radiation for the As analogue because the intensity data from the Guinier camera for the As analogue was too low to analyze for its phase purity. The powder diffraction pattern was compared with the calculated pattern based on the previously published single-crystal crystallographic data[13] and gave excellent agreement in 2θ positions and intensities.

Magnetization Measurement. The field- and temperature-dependent magnetization was measured on a commercial SQUID magnetometer (MPMS XL, Quantum Design). The temperature dependence was measured between 10 and 750 K for the As analogue and between 10 and 300 K for the Sb analogue under 10 000 Oe. The field-dependent magnetization was measured between 0 and 5 T at 195 and 360 K for the As analogue and 75 and 150 K for the Sb analogue to investigate the difference in magnetization above and below the T_c. For all the measurements, about 0.1 g of the sample was used, and it was sealed in a fused silica tube under a high vacuum to prevent its decomposition reaction with the air.

Powder Neutron Diffraction. The magnetic spin ordering and structural change of the $Na_2Ti_2Pn_2O$ system was investigated by powder neutron diffraction on the DUALSPEC diffractometer at the Chalk River Laboratories of AECL (Atomic Energy of Canada Limited). Diffraction patterns were acquired for both As and Sb compounds using a $\lambda = 2.3692$ Å wavelength neutron beam. The sample was enclosed in a vanadium tube sealed with an indium gasket. Temperature was controlled by a helium closed-cycle cryostat. The diffraction data were collected above and below the T_c of both compounds.

Electrical Transport Measurement. The electrical resistivity was measured by the four-probe method using a Quantum Design SQUID magnetometer (MPMS XL system). Platinum leads are attached to the cylindrical-shaped sintered sample of the approximate dimensions 2.8 mm (diameter) × 5 mm (length), using sodium metal as the contact material. The sample was placed on a LakeShore electrical property measurement holder, and it was coated with Kapton tape and UHU-epoxy to prevent its decomposition reaction with the air. The resistivity was measured between 10 and 360 K for the As analogue and between 10 and 300 K for the Sb analogue. Ohmic behavior was observed over the applied current range of 0.05−1.00 mA at room temperature, and the applied current of 0.10 mA was chosen for the temperature-dependent measurement for both compounds.

Results and Discussion

The powder X-ray diffraction results are shown in Figure 3 for the As analogue and the Figure 3 inset for the Sb analogue. The diffraction peaks are indexed according to the calculated pattern based on the previously published $Na_2Ti_2Pn_2O$ structure.[13] For the As analogue, all the peaks were indexed, except the two peaks at the 2θ positions, 32° and 41°, arising from the presence of a small amount of an unidentified phase. Among these peaks, the peak at 32° is found to increase in intensity as the sample oxidizes. For the Sb analogue, there was only one peak not indexed near 34°. When these samples are exposed to the air, they decompose to a darker gray phase in a few seconds and the volume of the sample increases by approximately a factor of 1.5.

Temperature-dependent dc magnetic susceptibility measurements were performed for both As and Sb compounds (Figure 4). The data show a drop in the susceptibility for both compounds; however, the Sb analogue exhibits a sharper drop than the As analogue. The As analogue has the T_c^{onset} (onset transition temperature) = 330 K, and the susceptibility gradually decreases as temperature decreases down to T_c^{min} (minimum susceptibility temperature) = 195 K (Figure

(38) *Film Scan: A Program for Digital Processing of Scanned Films, v.2.0*; Materials Data Inc.: Livermore, CA, 1999.
(39) *Jade: A Program for Diffraction Pattern Analysis and Phase Identification, v.5.0*; Materials Data Inc.: Livermore, CA, 1999.

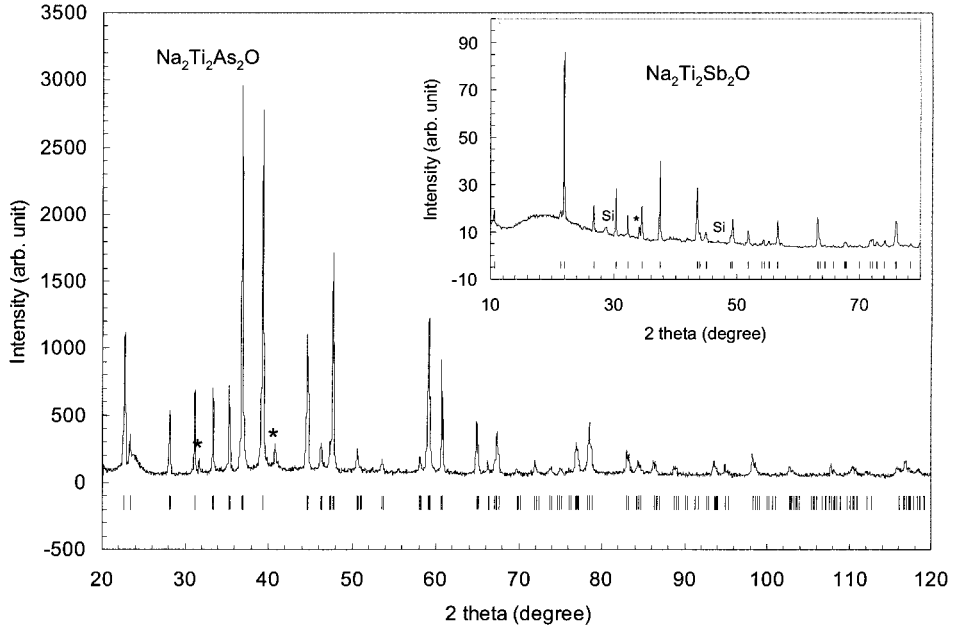

Figure 3. Powder X-ray diffraction pattern of $Na_2Ti_2As_2O$ and $Na_2Ti_2As_2O$ (inset). Solid line represents the experimental data and short vertical toggles represent calculated Bragg reflection positions. Asterisks indicate the experimental reflections that cannot be indexed based on the calculated diffraction pattern.

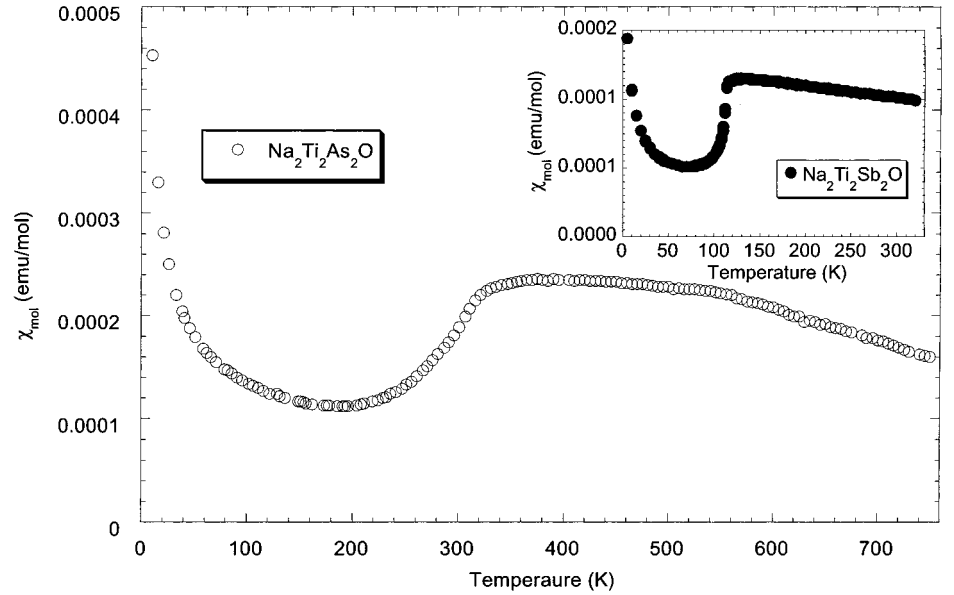

Figure 4. Temperature variation of dc magnetic susceptibility of $Na_2Ti_2As_2O$ and $Na_2Ti_2Sb_2O$ (inset) measured at 10 000 Oe.

4). On the other hand, the Sb analogue has the $T_c^{onset} = 120$ K, and the susceptibility decreases as temperature decreases down to $T_c^{min} = 75$ K (Figure 4 inset). Both compounds show no detectable differences between zero-field-cooled and field-cooled susceptibility, and the susceptibility decreases gradually above T_c^{onset} as temperature increases. In addition, Curie-like tails[40] were observed below their T_c^{min} for both compounds. These tails likely originate from a small fraction of paramagnetic impurity phase, and they are believed to be extrinsic to the $Na_2Ti_2Pn_2O$ for two reasons: First, the magnitude of the tails can be correlated with the phase purity of the sample and are sample-dependent. Second, upon exposure to the air, both As and Sb compounds decompose completely in a few seconds, and the susceptibility changes into simple Curie behavior.

Field-dependent magnetization at temperatures above and below the T_c of both As and Sb analogues is shown in Figure 5. For all the measurements, magnetization exhibits a linear dependence upon applied field, indicating the presence of no ferromagnetic impurity in the sample. For both compounds, magnetization above T_c is about a factor of 3 larger than that below the T_c at all applied fields, and no hysteresis behavior was observed in a field loop measurement.

To investigate the magnetic spin ordering and structural change, powder neutron diffraction was performed above and below the T_c for both compounds. The results are shown in Figure 6 for both As and Sb compounds. The data for the Sb compound are shown as an inset

(40) Gschneidner, K. A., Jr. *J. Magn. Magn. Mater.* **1985**, *47&48*, 57.

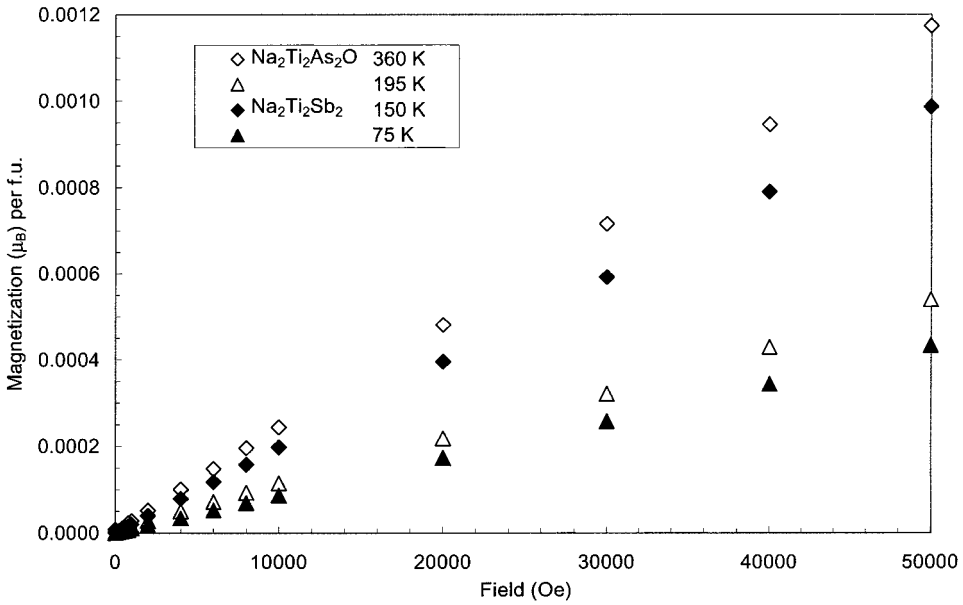

Figure 5. Magnetization versus applied field of $Na_2Ti_2As_2O$ and $Na_2Ti_2Sb_2O$ measured above and below their magnetic transition temperatures.

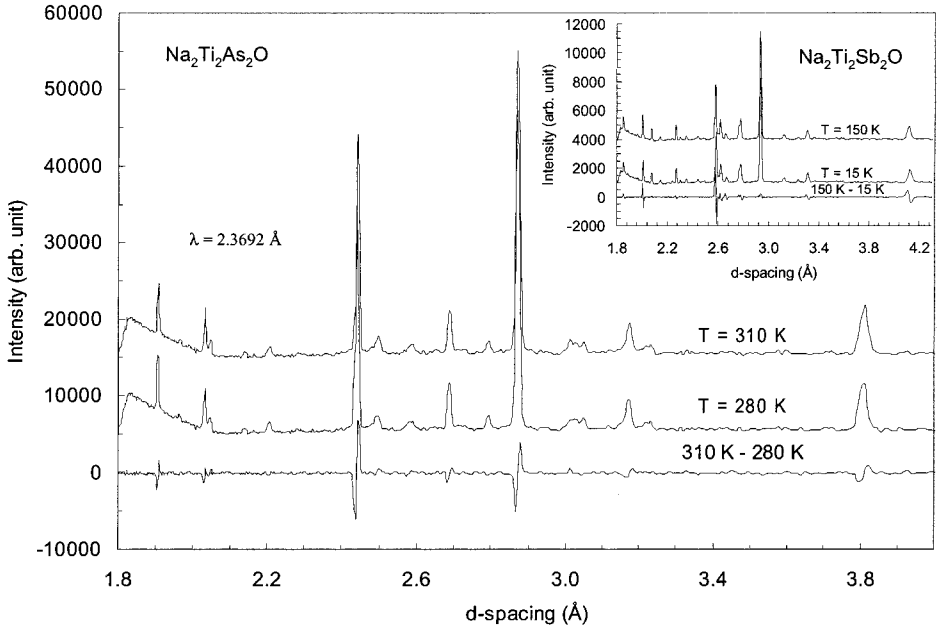

Figure 6. Powder neutron diffraction profiles of $Na_2Ti_2As_2O$ at 310 and 280 K along with their difference. The inset shows the powder neutron diffraction profiles of $Na_2Ti_2Sb_2O$ at 150 and 15 K along with their difference.

Table 1. Lattice Parameters of $Na_2Ti_2Pn_2O$ Obtained from Powder Neutron Diffraction

	a (Å)	*c* (Å)
$Na_2Ti_2As_2O$ at 280 K	4.0791(8)	15.316(2)
$Na_2Ti_2As_2O$ at 310 K	4.0810(9)	15.331(3)
$Na_2Ti_2Sb_2O$ at 15 K	4.161(2)	16.512(7)
$Na_2Ti_2Sb_2O$ at 150 K	4.160(2)	16.558(7)

because these data have previously been published.[20] This figure shows the diffraction profiles above and below the T_c as well as the profile difference between those. Lattice parameters were obtained from the indexed neutron diffraction peak positions and refined by the least-squares method (Table 1). One thing noticeable from these data is that, within their standard deviation, the lattice parameter *a* does not change above and below T_c whereas the lattice parameter *c* decreases below T_c. This observation agrees with previously proposed $^2T_{2g}$ Jahn−Teller-like distortion of Ti^{3+} coordination in the Sb analog[20] where the bond distance ratio of O−Ti−O/Sb−Ti−Sb increases below T_c. This distortion is commensurate, and the same symmetry is retained after the distortion. This commensurate distortion is unlike the conventional Peierls transition[41] for which the periodicity of the distorted lattice has an integral multiple of the undistorted lattice parameters with the multiplicity equal to or greater than 2. The signals observed in the difference plots (Figure 6) are only due to the shift in Bragg peaks that originated from the lattice parameter change, and no superlattice reflections due to magnetic spin ordering or symmetry breaking were observed for either compound. Thus, these

(41) Peierls, R. E. *Quantum Theory of Solids*; Clarendon Press: Oxford, 1955.

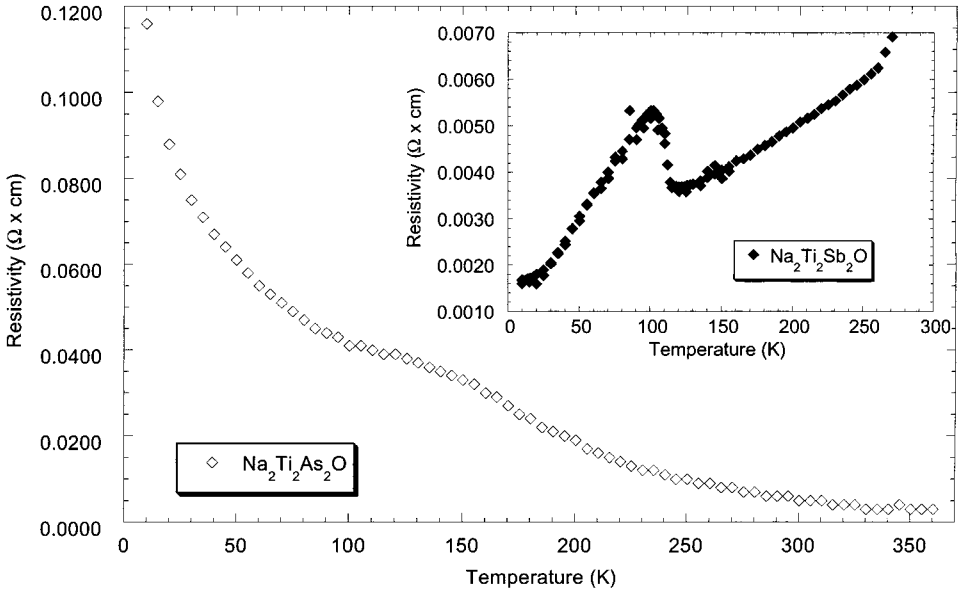

Figure 7. Electrical resistivity versus temperature of $Na_2Ti_2As_2O$ and $Na_2Ti_2Sb_2O$ (inset).

results indicate that the physical property anomaly is not likely arising from simple antiferromagnetic ordering or a spin-Peierls transition.

The result of the temperature-dependent electrical resistivity measurement exhibits the most pronounced difference between the As and Sb analogues. The As analogue exhibits an insulator-to-insulator transition at $T_c^{mid} = 135$ K (inflection point) (Figure 7). In contrast, the Sb analogue exhibits a metal-to-metal transition at $T_c^{mid} = 110$ K with $T_c^{onset} = 120$ K (Figure 7 inset), corresponding to the onset of the magnetic susceptibility anomaly. These behaviors are reminiscent of those in the quasi-two-dimensional CDW/SDW materials such as $TlMo_6O_{17}$[42] and $P_4W_{14}O_{56}$,[43] respectively, for metal-to-metal and insulator-to-insulator transitions. Below T_c, the resistivity increases for both the As and Sb analogues.

The *a* lattice parameter is smaller for the As analogue; therefore, Ti···Ti metallic interaction in the As analogue is expected to be greater than that in the Sb analogue. Thus, more metallic conductivity was expected in the As analogue. However, the electrical resistivity of the As analogue is higher than that of the Sb analogue by approximately a factor of 10. There are two hypotheses that can be used to explain the experimental results. First, because Sb orbitals are more diffuse, it is more metallic than As. Second hypothesis is that the physical property anomaly in these compounds is due to a CDW/SDW transition as predicted by the theoretical calculations.[34,35] The existence of a CDW/SDW in two-dimensional compounds is rare compared with that of the one-dimensional compounds because the Kohn anomaly of the phonon, a precursor of a CDW/SDW transition, in dimensions higher than one is much less pronounced than that of a one-dimensional system.[44] However, there are some examples of two-dimensional materials that exhibit CDW/SDW behavior such as tungsten[43,45,46] and molybdenum bronzes.[47−50]

The susceptibility decrease below T_c for both As and Sb compounds can qualitatively be explained in terms of gap opening at the Fermi surface caused by CDW/SDW instability.[43,51] The higher susceptibility above T_c is due to Pauli susceptibility originating from conduction electrons. The gap opening at the Fermi surface due to CDW/SDW instability causes a decrease in conduction electron concentration; thus, the magnetic susceptibility decreases below T_c. Similarly, the increase in resistivity at the T_c for both As and Sb compounds can be explained in terms of a decrease in conduction electron concentration caused by the gap opening by CDW/SDW instability.

The magnetic property differences between the As and Sb analogues can be rationalized in terms of the dimensionality of the compounds. A CDW/SDW is known to be suppressed as the dimensionality of the system increases. In the case of the $Na_2Ti_2Pn_2O$ system, the As analogue has a smaller interlayer distance than the Sb analogue. Thus, we can propose that the As analogue has stronger interlayer interaction and therefore more three-dimensional character than the Sb analogue. The Sb analogue has a more pronounced magnetic transition than the As analogue due to its higher CDW/SDW amplitude arising from its lower dimensionality. This CDW/SDW scenario is also supported by the previously published temperature-dependent powder neutron diffraction results of the Sb analogue. The diffraction results show that there is a structural distortion at the

(42) Ramanujachary, K. V.; Collins, B. T.; Greenblatt, M. *Solid State Commun.* **1986**, *59*, 647.
(43) Greenblatt, M. *Acc. Chem. Res.* **1996**, *29*, 219.
(44) Kagoshima, S.; Nagasawa, H.; Sambongi, T. *One-Dimensional Conductors*; Springer-Verlag: Berlin, 1988; p 22.
(45) Greenblatt, M. *Int. J. Mod. Phys. B* **1993**, *7*, 3937.
(46) Lehmann, J.; Schlenker, C.; Touze, C. L.; Rötger, A.; Dumas, J.; Marcus, J.; Teweldemedhin, Z.; Greenblatt, M. *J. Phys. IV* **1993**, *3*, 243.
(47) Buder, R. D. J.; Dumas, J.; Marcus, J.; Mereier, J.; Schlenker, C. *J. Phys. Lett.* **1982**, *43*, L59.
(48) Greenblatt, M.; Ramanujachary, K. V.; McCarroll, W. H. *J. Solid State Chem.* **1985**, *59*, 149.
(49) Greenblatt, M. *Chem. Rev.* **1988**, *88*, 31.
(50) Ganne, M.; Dion, M.; Boumaza, A.; Tournoux, M. *Solid State Commun.* **1986**, *59*, 137.
(51) Kagoshima, S.; Nagasawa, H.; Sambongi, T. *One-Dimensional Conductors*; Springer-Verlag: Berlin, 1988; p 102.

same temperature as the T_c of resistivity and magnetic susceptibility, providing the evidence for strong electron−phonon interaction. The electrical conductivity differences between the As and Sb analogues might be attributed to their electronic structure differences. The higher conductivity of the Sb analogue might be due to its better overlap of orbitals in the two-dimensional layer and a wider band relative to those of the As analogue.

In conclusion, bulk properties of $Na_2Ti_2As_2O$ and $Na_2Ti_2Sb_2O$ have been measured and anomalous transitions in the magnetic susceptibility and electrical resistivity reminiscent of a CDW/SDW have been discovered. The anomaly observed in the $Na_2Ti_2Pn_2O$ system is an indication of a new kind of two-dimensional CDW/SDW behavior. It is now of interest to confirm the existence of a CDW/SDW in these compounds because electron−phonon interactions of CDW/SDW materials are similar to those of superconductors and play central roles in anomalous and practical properties.[52] Pressure-dependent heat capacity measurement is underway because the heat capacity of CDW/SDW materials is known to be pressure-dependent.[44,53] Furthermore, angle-resolved photoemission experiments should be performed on a single-crystal sample. The theoretical calculation predicts that the Sb analogue compound has a strongly "nested" box-like Fermi surface, which induces the CDW/SDW instability.[34,35] Thus, a Fermi contour map produced from the photoemission result can be used to confirm the existence of the CDW/SDW.

Acknowledgment. We thank Warren E. Pickett for useful discussion, Robert N. Shelton for the use of the SQUID magnetometer and X-ray diffractometer, and Peter Klavins for assistance with instrumentation. This research is supported by NSF DMR-9803074 and the Natural Sciences and Engineering Research Council of Canada. We also acknowledge the Neutron Program for Materials Research of the National Research Council of Canada, which operates the DUALSPEC instrument at the Chalk River Nuclear Laboratory.

CM010009F

(52) Fröhlich, H. *Proc. R. Soc. London* **1954**, *A223*, 296.
(53) Tang, J.; Matsumoto, T.; Abe, H.; Matsushita, A. *Solid State Commun.* **1999**, *109*, 445.